

# Multi-decadal scale variability in autumn-winter rainfall in south-western Australia since 1655 AD as reconstructed from tree rings of *Callitris columellaris*

Louise E. Cullen · Pauline F. Grierson

Received: 4 March 2008 / Accepted: 14 August 2008 / Published online: 9 September 2008  
© Springer-Verlag 2008

**Abstract** We present the first tree-ring based reconstruction of rainfall for the Lake Tay region of southern Western Australia. We examined the response of *Callitris columellaris* to rainfall, the southern oscillation index (SOI), the southern annular mode (SAM) and surface sea temperature (SST) anomalies in the southern Indian Ocean. The 350-year chronology was most strongly correlated with rainfall averaged over the autumn-winter period (March–September;  $r = -0.70$ ,  $P < 0.05$ ) and SOI values averaged over June–August ( $r = 0.25$ ,  $P < 0.05$ ). The chronology was not correlated with SAM or SSTs. We reconstructed autumn-winter rainfall back to 1655, where current and previous year tree-ring indices explained 54% of variation in rainfall over the 1902–2005 calibration period. Some variability in rainfall was lost during the reconstruction: variability of actual rainfall (expressed as normalized values) over the calibration period was 0.78, while variability of the normalized reconstructed values over the same period was 0.44. Nevertheless, the reconstruction, combined with spectral analysis, revealed that rainfall naturally varies from relatively dry periods lasting to 20–30 years to 15-year long periods of above average rainfall. This variability in rainfall may reflect low-frequency variation in the El Niño-Southern Oscillation rather than the effect of SAM or SSTs.

**Keywords** Cupresseaceae · Dendroclimatology · Semiarid Australia · El Niño southern oscillation

## 1 Introduction

It has become increasingly apparent that climate change is significantly influencing hydrological regimes. Globally, rainfall has increased by nearly 1% per decade over the twentieth century (New et al. 2001) such that many regions are now experiencing their wettest ever conditions. For example, rainfall in northern Pakistan was greater during the twentieth century than at any time during the last millennium (Treydte et al. 2006). However, rainfall over the last 100 years has declined, rather than increased, in a number of regions, including the African Sahel, the Mediterranean, southern Africa and parts of southern Asia (e.g. Sarris et al. 2007; Solomon et al. 2007). Similarly, since the late 1960s the south-west of Western Australia (SWWA; Fig. 1) has experienced a sustained decline in winter rainfall of around 20% relative to average rainfall since 1911 (Hennessy et al. 1999; Nicholls and Lavery 1992; Smith 2004). This decline in rainfall has affected not only agricultural productivity, but also recharge to regional water supplies (IOCI 2002). For example, annual streamflow into dams that supply the Perth metropolitan area has declined by 50% since 1975 (Pittock 2003). Furthermore, current predictions based on climatological models suggest winter rainfall will continue to decline, perhaps by as much as 60% by 2070 AD (CSIRO 2001).

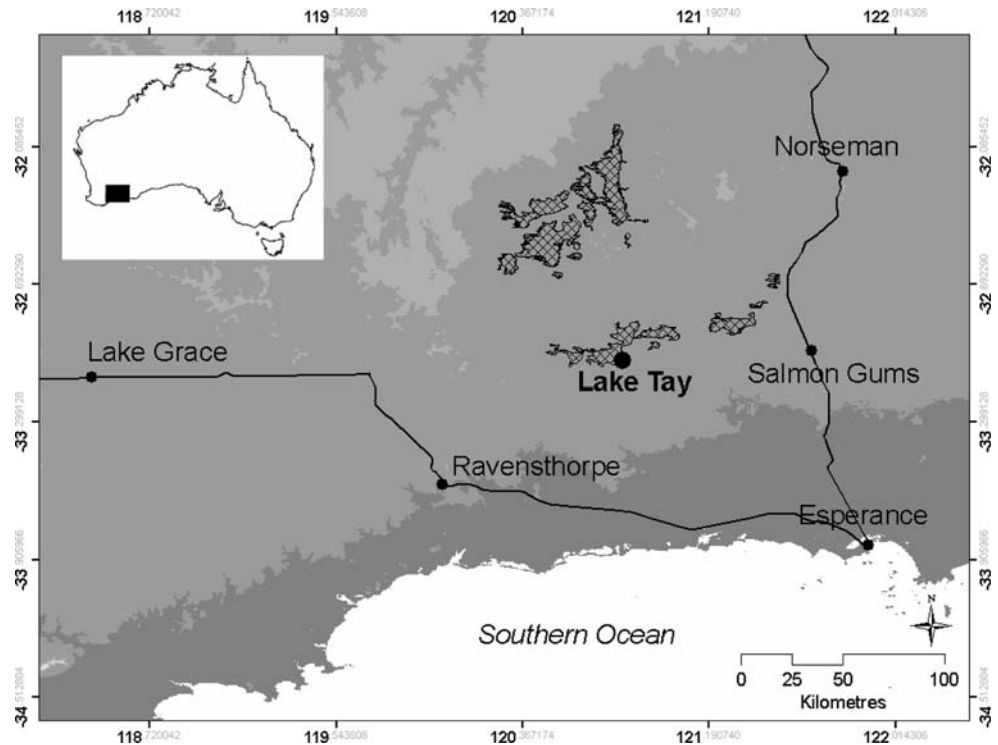
Several studies have attempted to identify the causes of the recent decline in SWWA rainfall. Using instrumental records, the decrease in rainfall has been correlated with a decrease in the density of low-pressure systems in the region and increase in mean sea level pressure (Ansell et al.

---

L. E. Cullen · P. F. Grierson (✉)  
Ecosystems Research Group, School of Plant Biology M090,  
University of Western Australia, 35 Stirling Highway,  
Crawley, WA, Australia  
e-mail: pfgblue@cylle.uwa.edu.au

L. E. Cullen  
e-mail: loucullen@farmside.co.nz

**Fig. 1** Map showing location of Lake Tay study site. A 90 m Digital Elevation Model is shown with grayscale shading for the categories 0–200 (darkest gray), 201–400, 401–600, 601–1,200 m (white). Lakes with an area greater than 5 km squared are hatched. Major roads are shown with black lines. Ticks show latitude and longitude in decimal degrees in the WGS84 map datum



2000; Smith et al. 2000). In particular, the development of low pressure systems over southern Australia was around 33% weaker during 1975–1994 compared with 1949–1968 (Frederiksen and Frederiksen 2005). In addition to these studies, climate models have been able to reproduce recent changes in rainfall of SWWA by including increases in atmospheric CO<sub>2</sub> (e.g. Cai et al. 2003; Kushner et al. 2001). In contrast, simulations using the CSIRO Mark 3 climate model without any CO<sub>2</sub> increase (Gordon et al. 2002), concluded that at least part of the observed rainfall decline was likely due to natural climate variability (Cai et al. 2005). Two aspects of the Southern Hemisphere atmospheric circulation system, the southern annular mode (SAM) and the El Niño-southern oscillation (ENSO), have been promoted as drivers of natural variability in rainfall over the region at the multi-decadal scale (IOCI 2002; Li et al. 2005; Smith et al. 2000). More recently, however, Samuel et al. (2006) found that winter rainfall in the region was related to sea surface temperatures (SSTs) over two specific areas of the Indian Ocean, the tropical western and southern Indian Ocean. Their study also suggested that the recent decline in rainfall was due to a step change in Indian Ocean SSTs (Samuel et al. 2006).

Uncertainty as to what drives rainfall variation over southern Western Australia in general, and the SWWA region more specifically, reflects both the relative shortness of instrumental records available, which are usually less than 100 years in length (Bureau of Meteorology 2001), and the need to benchmark data from climate models

against independent records of climate (Jones et al. 1998). In particular, generating climate records of multi-centennial to millennial length is crucial to understanding the extent and cause of natural variability in rainfall. For example, it was only through the development of hydroclimatic records spanning the last millennium that evidence for ‘megadroughts’ lasting several decades or more in western North America became apparent; during the period with instrumental data no drought had lasted longer than 10 years (Graham et al. 2007; Seager et al. 2007). Similarly, a millennial length reconstruction of rainfall for northern Pakistan using oxygen isotope records from tree rings revealed centennial-scale variations in rainfall (Treydte et al. 2006). Examination of variability in long time series is also relevant to questions about whether apparent shifts in climatic regimes are spurious ‘red noise’ processes (e.g. Rodionov 2006).

Extending climate records back several centuries or longer to provide baseline data relies on natural archives. However, there has been almost no effort given in Australia to developing accurately dated rainfall proxies, despite the high spatial and temporal variability in rainfall across the continent. Indeed, for all of Australia, there appears to be just one multi-centennial length reconstruction of rainfall: coral luminescence was used to reconstruct rainfall for eastern Queensland from 1631 to 1983 AD (Lough 2007). While calcite layers in speleothems from caves in Western Australia have shown promise as a rainfall proxy (Treble et al. 2003, 2005), this method is currently limited by

uncertainties over its temporal resolution. In contrast, for southern Western Australia the annual growth rings of trees of the native Australian conifer *Callitris* (Cupressaceae) have significant potential as climate proxies (Cullen and Grierson 2006, 2007; LaMarche et al. 1979).

Several studies have demonstrated that tree-rings of *Callitris* reflect variation in rainfall (e.g. Ash 1983; Lange 1965). For example, Ash (1983) reported a correlation of 0.52 between annual rainfall and tree-ring widths of tropical *C. macleayana*, while rainfall explained 70% of the variation in ring widths of *C. columellaris* in the eastern goldfields of WA (Perlinski 1986). The results of these early studies indicate *Callitris* has potential to provide information on natural variability in rainfall for much of Australia as the genus occurs across the continent, particularly in semi-arid or strongly seasonal climates. Here, we have tested the dendroclimatic potential of *Callitris* in southern WA by developing a 350-year reconstruction of autumn–winter (May–September) rainfall using tree rings of *C. columellaris* F. Muell. We then used this reconstruction to investigate multi-decadal scale variation in rainfall for the Lake Tay area, which lies on the eastern boundary of the SWWA region. We also examined the relationship between our tree-ring chronology and ENSO, SAM and SSTs in the southern Indian Ocean in order to clarify the main forcing mechanisms driving multi-decadal rainfall variability.

## 2 Data and methods

### 2.1 Study site

For our study, we selected a large stand of *C. columellaris* (formerly described as *C. glaucophylla*, now considered a taxonomic synonym of *C. columellaris*; Farjon 2005) trees growing on the south-western edge of Lake Tay, in southern Western Australia (33°1'57"S, 120°45'9"E; Fig. 1). Owing to extensive land clearance within the SWWA, there are no suitable stands of *Callitris* within the main area that has experienced a decline in rainfall over recent decades. The study area is in a region thought to have shown little or no change in rainfall patterns over recent decades (Fig. 4a), and is ~200 km to the east of the boundary of the SWWA region. Nevertheless, our study contributes much needed data on long-term climate variability for southern Western Australia.

Scattered and relatively large (>20 cm diameter) trees of *C. columellaris* are dominant on the low-lying gypsum dunes adjacent to Lake Tay. Climate is semi-arid and strongly seasonal with dry, warm summers and cool, wet winters. Mean annual rainfall is around 240 mm, 70% of which falls between March and September (autumn

through winter). Daytime temperatures range from nearly 30°C in summer (December–February) to 16°C in July. Maximum rates of tree growth and annual ring formation are likely to occur, therefore, during the Southern Hemisphere winter and spring period with dormancy by late summer.

### 2.2 Chronology development

In March and April 2006, two to three 5 mm diameter cores were extracted from each of 30 trees at Lake Tay, with discs cut from four dead trees using a chainsaw. Cores and cross-sections were sanded using paper up to 1,200 grit. Heavy resin staining, which obscured ring boundaries, was removed by repeatedly heating the wood and wiping away excess resin. Visual crossdating and measuring accuracy was checked using Verify for Windows (Lawrence and Grissino-Mayer 2001) and COFECHA (Holmes 1983). The average series intercorrelation in COFECHA was relatively high at 0.67.

We developed our tree-ring width chronology using a two-step standardisation procedure in ARSTAN40c (Cook and Krusic 2006). Prior to detrending, we stabilised the variance of each ring-width series using a data-adaptive power transformation based on the local mean and standard deviation (Cook and Peters 1997). Non-climatic trends were removed from each series using cubic splines with a 50% response frequency cut-off equal to 67% the length of the series (67% N) (Cook and Briffa 1990). Given that the mean series length was 235 years, our detrending procedure captured multi-decadal to annual frequencies, but multi-centennial trends were removed. Tree-ring indices were calculated as differences (Cook and Peters 1997), while autocorrelation unique to each individual series was removed using the first-minimum Akaike Information Criterion (Cook 1985). However, autocorrelation common to all series, assumed to be related to climate (Cook 1985), was re-incorporated into each series. Series were then averaged using the bi-weight robust mean (Cook and Briffa 1990) and the variance of the chronology was stabilised with a 67% N spline to minimise the effect of changing sample size and other variables that cause variance to be time dependent (Osborn et al. 1997).

We used the chronology incorporating the common persistence (ARS chronology) for subsequent analysis of climate-growth relationships and reconstruction of rainfall rather than the standard (STD) chronology, in which autocorrelation unique to each series is retained, or the residual (RES) chronology, in which all autocorrelation is removed through autoregressive modelling, for several reasons. Removal of *all* autocorrelation may remove the long-term trends and variance potentially related to climate (Graumlich 1991; MacDonald et al. 1998) that are the

focus of our study. Climate often exhibits year-to-year persistence that generates low-frequency trends in tree growth (Cook and Briffa 1990). In recognition of this, previous studies interested in low-frequency climate variation have used the STD chronology (e.g. Knapp et al. 2001). However, the persistence contained within the STD chronology is likely to be related not only to climate but also the effects of disturbance (Cook and Briffa 1990). Selecting the ARS chronology for analysis of climate-growth relationships should provide, therefore, a balance between retaining long-term trends related to climate and dampening long-term trends related to non-climatic processes. Nevertheless, since there are few published chronologies for *Callitris*, we have included the commonly reported statistics for all three chronology types for comparison with other species (Table 1).

### 2.3 Growth-climate relationships in *C. columellaris*

To evaluate the climate signal contained in the Lake Tay chronology, we constructed a regional rainfall series (1902–2005) using climate data recorded at the three closest Australian Bureau of Meteorology (BOM) stations at Ravensthorpe (1902–current), Norseman (1897–current) and Salmon Gums (1933–current; Fig. 1). Climate data were checked for homogeneity by the BOM. Monthly rainfall at each station was normalized, relative to each station's mean and standard deviation, and then averaged. We also calculated normalized seasonal (summed over March–May, June–August and March–September) and total annual rainfall values. The regional rainfall series covers 1902–2005, the period for which there is a minimum of two data series.

In addition to the rainfall data, we accessed five climate indices that capture different aspects of the Southern Hemisphere atmospheric-circulation system. These indices were: (1) the Climatic Research Unit's Southern Oscillation Index (SOI) (1866–current), which is defined as the

normalized pressure difference between Tahiti and Darwin and calculated based on the method described in Ropelewski and Jones (1987); (2) sea surface temperature (SST) anomalies for the Niño 4 region (1950–current), which were accessed from the National Oceanic and Atmospheric Administration; (3) the southern annular mode (SAM, 1957–current), calculated as the difference in mean sea level pressure anomalies between six climate stations near 40°S and six climate stations near 65°S (Marshall 2003) and; (4) SST anomalies averaged over the two regions of the Indian Ocean identified by Samuel et al. (2006) has having influence on rainfall, the southern (60–70°E, 25 to 35°S) and tropical western (50–70°E, 10°S to 10°N) regions, which were accessed from the Kaplan Extended SST dataset (1856–current). For all climate indices, we calculated seasonal (March–May, June–August and March–September) and annual average values.

Relationships between our Lake Tay ARS chronology and monthly and seasonal climate data were examined using bootstrapped correlation analysis in DendroClim2002 (Biondi and Waikul 2004). Months and seasons from the preceding and current growth year were used in the analysis. DendroClim2002 uses 1,000 bootstrapped samples (drawn at random with replacement) to compute a median correlation coefficient for each month or seasonal variable. The median coefficient is considered to be significant at the 0.05 level if its absolute value exceeds half the difference between the 97.5th and 2.5th quantile of the 1,000 samples (Biondi and Waikul 2004).

### 2.4 Rainfall reconstruction

Growth–climate analysis indicated that tree growth was most strongly correlated with rainfall over the March–September period. To develop a linear regression between the ARS chronology and March–September rainfall, with the aim of reconstructing autumn–winter rainfall, we used a split calibration/verification procedure (Fritts 1976; Fritts

**Table 1** Descriptive statistics for the three *C. columellaris* chronology types: standard, STD; residual, RES; and arstan, ARS

No. of trees/cores	Time span <sup>a</sup>	Missing rings (%)	Chron. type	MS	SD	AC1	AR model	EPS	Mean correl.	Var (%)
11/15	1654–2005 (4)	1.62	STD	0.341	0.345	0.364	2	0.947	0.543	57.7
			RES	0.368	0.307	0.023	–	0.950	0.560	59.1
			ARS	0.331	0.333	0.357	2	–	–	–

Mean sensitivity (MS) is a measure of the relative change in ring-width from one year to the next. Standard deviation (SD) is about the mean index value (scaled to be 1.0). AC1 is the first order serial correlation, while AR model is the autoregressive process selected by the Akaike Information Criterion to remove autocorrelation. Mean correl. is the average correlation between all series. Var (%) is the percentage variance explained by the 1st eigenvector of a PCA. EPS is the expressed population signal, which quantifies the degree to which the chronology represents the hypothetically perfect chronology. Mean correl., Var (%) and EPS were calculated for the period common to all series, 1841–1960. Mean correl., EPS and Var (%) are not produced for the ARS chronology

<sup>a</sup> The Lake Tay chronology was cut at the point where sub-sample signal strength (Wigley et al. 1984) reached 0.85, number in parentheses indicates number of series from this point

et al. 1990). The regional rainfall series and ARS chronology were divided into two periods, 1902–1953 and 1954–2005. For each period, chronology indices from the current year ( $t$ ) and previous year ( $t - 1$ ) were used as the predictor for normalized rainfall (calibration). For both calibration models, including indices from the previous year increased the explained variation in rainfall and only these results are presented here. The regression coefficients from the calibration period were then used to transform the chronology indices from the second period into estimates of normalized rainfall for comparison with the observed data (verification). The verification statistics used were: Durbin–Watson statistic (Durbin and Watson 1951); Pearson’s correlation coefficient; Reduction of Error statistic; the coefficient of efficiency (CE) statistic; the sign test, calculated as departures from the means of the actual and reconstructed data; and product means test (Cook et al. 1994; Fritts et al. 1990).

## 2.5 Spectral analysis

Spectral analysis identifies recurrent features or periodicities in time series by expressing the variance of the series as a function of frequency. We used the multi-taper method (MTM) of spectral analysis (Thomson 1982), with robust estimation of the red-noise background (Mann and Lees 1996) to identify significant peaks in the spectra of the reconstructed and actual rainfall series for the period common to both (1902–2005) and for the full length reconstruction of rainfall. We conducted all spectral

analysis in k-Spectra V2.4 (Spectraworks) and the MTM spectra are based on five 3- $\pi$  tapers. Our aim in conducting the spectral analysis was to provide support to our visual interpretation of decadal or longer trends in the chronology rather than extensively explore its spectral properties.

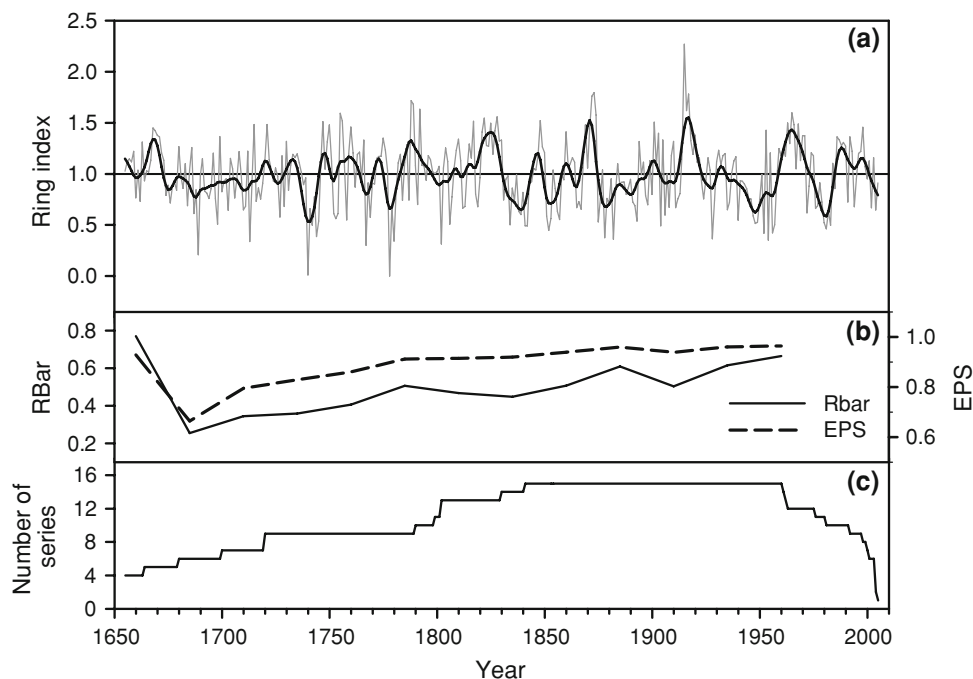
## 3 Results

### 3.1 The Lake Tay chronology

Crossdated measurements extended back to 1601 AD. However, we cut the Lake Tay chronology at 1654 AD (Fig. 2; Table 1), where the sub-sample signal strength (SSS) fell below 0.85 (Wigley et al. 1984). Sub-sample signal strength is a measure of the maximum useful length of a tree-ring chronology in terms of acceptable loss of reconstruction accuracy (Wigley et al. 1984). Individual tree ages ranged from 160 to 397 years, while the average age of trees included in the chronology was 235 years.

Removal of autocorrelation, or the addition of common persistence, had little effect on the statistics commonly used to assess chronology quality (Table 1). The residual (RES) Lake Tay chronology (containing no autocorrelation) had a slightly higher mean sensitivity (MS) and lower standard deviation than the standard (STD) or ARS chronologies. MS is a measure of high-frequency variation and climatic responsiveness, while standard deviation reflects the amount of low-frequency variation in a chronology (Fritts 1976). The difference in mean sensitivity and

**Fig. 2** **a** Tree-ring width chronology (with autocorrelation common to all series re-incorporated before averaging) developed from *Callitris columellaris* at Lake Tay, southern Western Australia. Annual values are plotted in *gray* and a 10-year smoothing spline in *black*. **b** RBar and EPS (Expressed Population Signal) values calculated for 50 year spans, each overlapping by 25 years. **c** Number of series included in the chronology over time. Chronology was cut at 1654, the year when the sub-sample signal strength fell below 0.85



standard deviation between the RES and STD or ARS chronologies is consistent, therefore, with the greater high-frequency (year-to-year) variation in the RES chronology due to the removal of lagged growth effects. The variance due to autocorrelation in the ARS chronology is 15.7%.

A strong common signal is evident for the STD and RES chronologies, with mean correlations between all series of  $>0.54$  and nearly 60% of variation explained by the first principal component (Table 1). Similarly, expressed population signal (EPS), a measure of the statistical quality of a chronology, was overall well above the 0.85 threshold commonly used to define reliability for both the STD and RES chronology (Table 1) (Briffa 1984). The running values of RBar and EPS dip in the late 17th century, possibly reflecting the relatively low number of cores included in the early part of the chronology (Fig. 2). However, after 1750 AD, EPS was consistently above 0.85.

### 3.2 Correlations with climate

The Lake Tay ARS chronology was more strongly correlated with annual or seasonal rainfall (all  $r > 0.46$ ) than with individual months (all  $r \leq 0.35$ ; Fig. 3). Of the various seasons tested, the chronology was most strongly correlated with rainfall from March–September (autumn–winter) of the current growing year ( $r = 0.70$ ,  $P < 0.05$ ; Fig. 3). The positive relationship between tree-ring widths and rainfall indicates low rainfall reduces tree growth, as expected for a semi-arid environment (Fritts 1976). No correlations with March–September rainfall, or any other season or month, from the preceding year were significant.

The Lake Tay ARS chronology was significantly correlated with the annual, June–August (winter) and March–September (autumn–winter) values of the SOI for the current growth year (Table 2). No other correlations between the chronology and the annual or seasonal values of the five climate indices were significant, although occasionally individual months were significant (not shown).

### 3.3 Rainfall reconstruction

The calibration models developed from the early (1902–1953) and late (1954–2005) periods explained over 50% of the variation in the regional rainfall series (Table 3). However, only the regression model from the late period passed all the verification tests. Predicted rainfall during the 1902–1953 verification period was significantly correlated with observed rainfall ( $P < 0.001$ ), with 57% of the variation in observed rainfall explained by the model (Table 3). The Durbin–Watson statistic (Durbin and Watson 1951) indicates that the residuals from the regression are neither positively nor negatively autocorrelated ( $P = 0.05$ ,  $n = 50$ ,  $d_L = 1.503$ ,  $d_U = 1.585$ ). In addition, the sign and product mean tests were significant at the 0.001 level. Both the reduction of error (RE) and coefficient of efficiency (CE) values were positive, indicating that the regression model had reasonable skill in predicting rainfall (Cook et al. 1994; Fritts 1976).

In contrast, the regression model from the early period (1902–1953) passed only some of the verification tests (Table 2). The correlation between predicted and observed

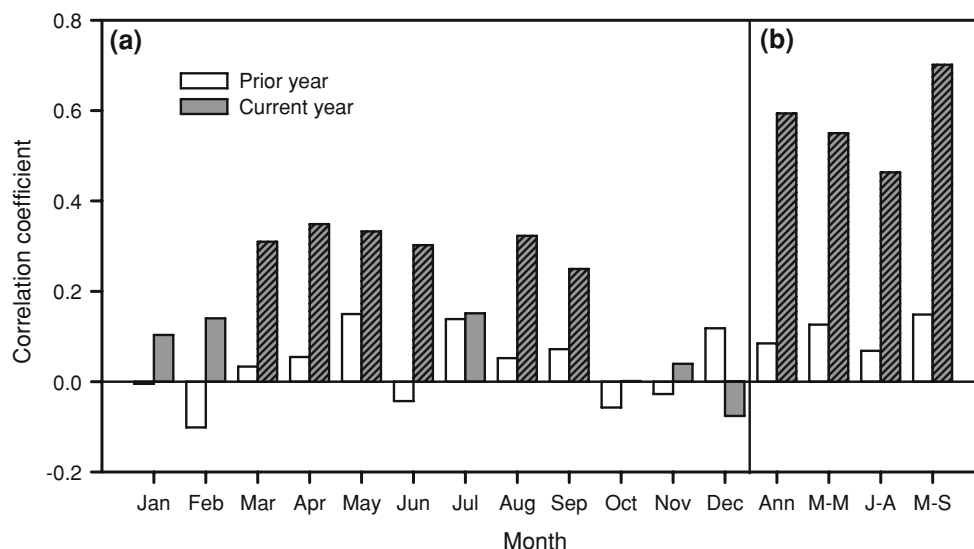


**Fig. 3** Bootstrap correlations between the Lake Tay ARS chronology and (a) monthly and (b) seasonal rainfall anomalies for both the year prior to growth (white bars) and current growth year (gray bars).

Seasons are: Annual (Ann), March–May (M–M), June–August (J–A) and March–September (M–S). Hatched bars indicate significant correlations ( $P < 0.05$ ).

**Table 2** Bootstrapped correlations between the Lake Tay ARS chronology and five climate indices: Climatic Research Unit's southern oscillation index (SOI), sea surface temperature anomalies in the Nino 4 region (Nino4), the southern annular mode (SAM), sea surface temperature anomalies in the southern Indian Ocean (SI-SSTs) and tropical western Indian Ocean (TWI-SSTs)

Correl. period Season	Climate index				
	SOI 1866–2005	Nino4 1950–2005	SAM 1957–2005	SI-SSTs 1856–2005	TWI-SSTs 1856–2005
Previous year					
Annual	0.03	0.08	−0.14	−0.08	0.05
Mar–May	−0.05	0.14	0.01	−0.04	0.08
Jun–Aug	0.11	0.04	−0.24	−0.08	0.04
Mar–Sept	0.06	0.08	−0.16	−0.06	0.07
Current year					
Annual	<b>0.20</b>	−0.13	−0.10	−0.09	−0.07
Mar–May	0.10	−0.13	−0.04	−0.05	−0.10
Jun–Aug	<b>0.25</b>	−0.08	−0.08	−0.13	−0.07
Mar–Sept	<b>0.21</b>	−0.11	−0.07	−0.09	−0.09

Correlations are presented for the average annual values and averages calculated for March–May, June–August and March–September for both the current growth year and the previous year. Correlation values in bold were significant ( $P < 0.05$ )

**Table 3** Calibration and verification statistics for a reconstruction of March–September rainfall using the ARS chronology developed from Lake Tay

Calibration period	1902–1953	1954–2005	1902– 2005
Verification period	1954–2005	1902–1953	–
<i>n</i>	51	51	103
Calibration			
<i>r</i>	0.71***	0.75***	0.73***
Adj. $r^2$	0.50	0.57	0.54
Durbin–Watson	1.66	1.63	1.63
Verification			
<i>r</i>	0.75***	0.71***	–
Adj. $r^2$	0.57	0.51	–
Durbin–Watson	1.69	1.66	–
Sign test (agree/disagree)	37/14***	42/9***	–
PM test (mean +ve/mean - ve)	0.61/ 0.08***	0.57/ 0.11***	–
Reduction of error	−0.11	0.31	–
Coefficient of efficiency	−0.12	0.31	–
Regression coefficients			
Ring-index ( <i>t</i> )	1.878	2.257	2.071
Ring index ( <i>t</i> − 1)	−0.460	−0.945	−0.697
Intercept	−1.432	−1.261	−1.358

The final regression model used for reconstruction was fitted over the full period (1902–2005)

\*\*\*Significant at the 0.001 level

rainfall over the 1954–2005 verification period was significant ( $P < 0.001$ ), with 51% variation explained, and the sign and product means tests were also significant ( $P < 0.001$ ). Again, the Durbin–Watson statistic indicates

that the residuals from the regression are neither positively nor negatively autocorrelated ( $P = 0.05$ ,  $n = 50$ ,  $d_L = 1.503$ ,  $d_U = 1.585$ ). Although the regression model passed these less rigorous tests, both RE and CE were negative (Table 3). Negative values for these statistics indicate that the regression model from the early period failed to predict rainfall with any accuracy (Cook et al. 1994; Fritts 1976). However, neither RE nor CE have a lower bound and, consequently, one or two extremely bad estimates can force them below 0. For example, the negative RE and CE values obtained using the regression model from the early period appears to reflect poor reconstruction of rainfall for just two years, 1992 and 2005. When these years are removed from the verification period, RE and CE change to 0.38 and 0.37.

The regression coefficients ( $P = 0.316$  for ring-index (*t*) and  $P = 0.199$  for ring-index (*t* − 1)) and intercepts ( $P = 0.596$ ) from the early and late calibration periods were not significantly different (Table 3). This similarity in regression equations, coupled with the improved verification of the early period with the removal of 1992 and 2005, indicates that a regression equation using the full 1902–2005 period can be used to reconstruct rainfall. A regression model using the full period explained 54% of the variation in rainfall (Table 3). In addition, actual rainfall for March–September and that reconstructed using the regression model from the full period show very good congruency (Fig. 4a). On the whole, the regression model reconstructs not only year-to-year changes in rainfall well, but also longer-term trends. There was no linear trend in the difference between predicted and actual rainfall ( $P = 0.114$ , adj.  $r^2 = 0.01$ ; Fig. 4b), while a 21-year

**Fig. 4** **a** Actual and reconstructed autumn–winter (March–September) rainfall for 1902–2005 using the Lake Tay ARS chronology, **(b)** residuals, or difference between predicted and actual rainfall, **(c)** 21-year running correlation between actual and reconstructed rainfall, plotted in the middle of each period, with the 0.05 significance level

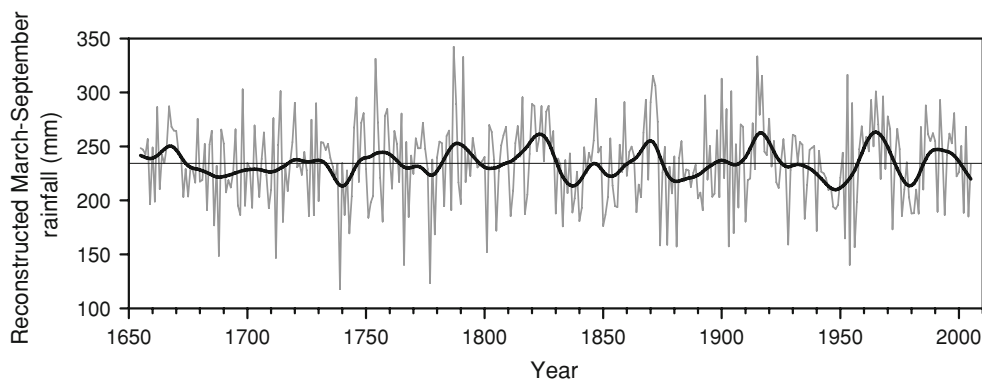
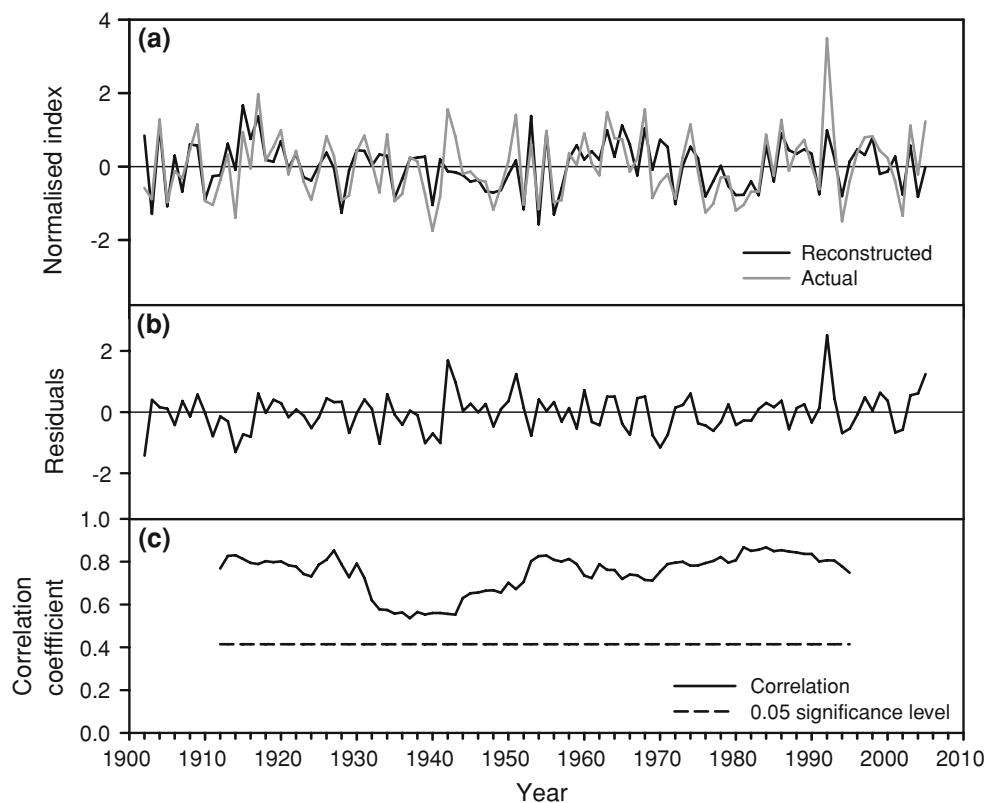


**Fig. 5** Reconstructed autumn–winter (March–September) rainfall from 1655 to 2005, scaled to the mean and standard deviation of the regional rainfall series for 1902–2005. Annual values are plotted in *gray* and a 20-year smoothing spline in *black*. The fitted smoothing

spline is designed to emphasise variation occurring at the scale of 20 years or longer. The mean of the reconstructed rainfall series is  $234.28 \pm 38.0$  mm

running correlation between actual and reconstructed rainfall was always significant ( $P < 0.05$ ; Fig. 4c). Consequently, we used the model from the full period to reconstruct rainfall for the autumn–winter (March–September) period back to 1655 AD (Fig. 5). We note, however, that the reconstruction of rainfall does not capture the full variability of the actual data series: variability of the normalized regional rainfall series from 1902 to 2005 was 0.78, whereas variability of the normalized reconstruction of rainfall for the same period was 0.44.

### 3.4 Multi-decadal variability in autumn–winter rainfall

Over the last 350 years autumn–winter rainfall has varied substantially at the multi-decadal scale (Fig. 5). Based on the 20-year spline fitted to the annual values, which emphasises lower frequency variability, periods of above average rainfall occurred 1660–1675, 1785–1800, 1815–1830, 1910–1925 and 1960s to mid 1970s (Fig. 5). An extended period of slightly below average rainfall occurred from 1675 to around 1715, with periods of dry conditions



also from 1735–1745, 1830–1860, 1875–1895, 1925–1955 and 1975–1985 (14 mm below average). The 1940s to early 1950s was the driest period of the last 350 years, when rainfall was 18 mm below the long-term average. In contrast, the 1820s were the wettest; rainfall was around 23 mm above average.

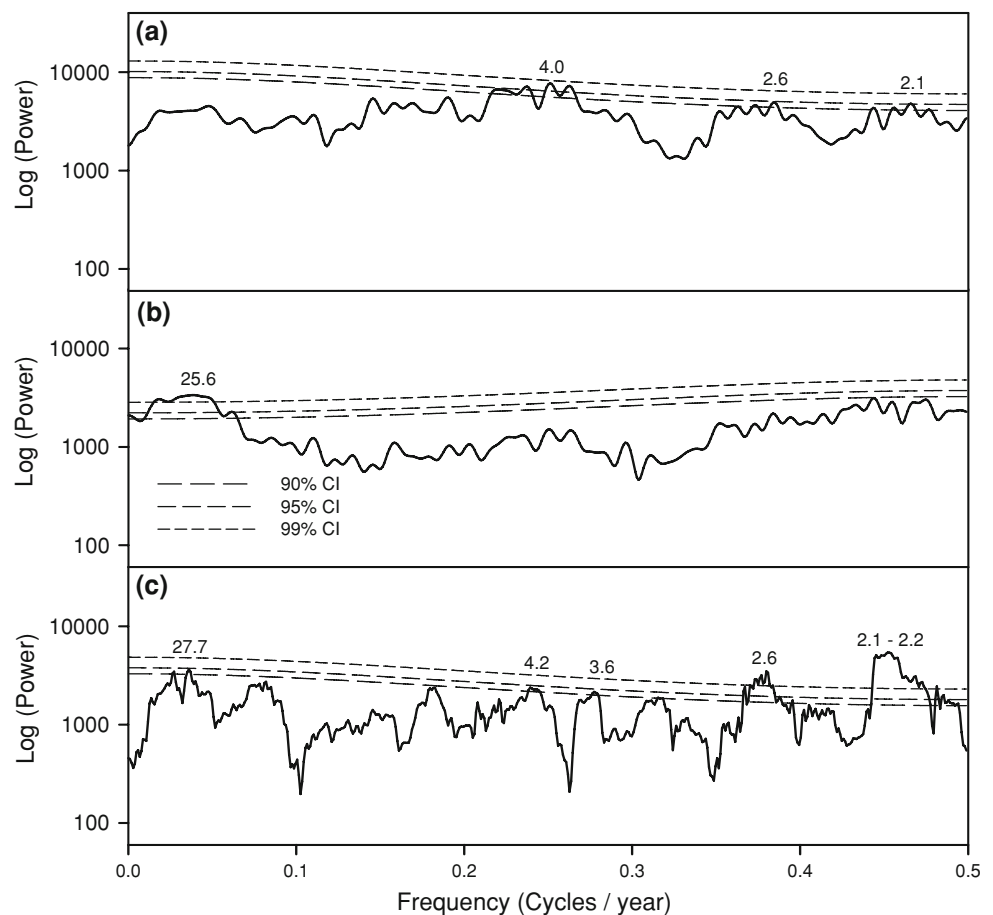
The MTM spectral analysis of the rainfall reconstruction also provides evidence for variability in rainfall operating at the multi-decadal and inter-annual scale (Fig. 6). Significant peaks (exceeding the 95 and 90% confidence levels) at periodicities of 2.1 and 2.6 years were identified from the actual rainfall series (Fig. 6a). Although spectral analysis of the rainfall reconstruction over the same 1902–2005 period did not detect this high frequency component (Fig. 6b), significant peaks (at the 99% confidence level) were identified in the full-length (1655–2005) reconstruction of rainfall at periodicities of 2.1 and 2.6 years (Fig. 6c). Furthermore, the spectral analysis indicates a significant peak in the full-length reconstructed and actual rainfall series in the 3.6–4.2 year bandwidth. Notably, the spectrum of the rainfall reconstruction also suggests a low frequency component: spectral analysis of the 1902–2005 portion of the rainfall reconstruction detects a broad and significant peak (at the 99% level) centred at a periodicity

of 26 years (Fig. 6b), while there is also a significant peak (at the 90% level) at 27.7 years in the spectrum of the full rainfall reconstruction (Fig. 6c). This peak was not evident from the actual rainfall data.

#### 4 Discussion

Our reconstruction extends available data on past rainfall for southern Western Australia by threefold and is a significant development for palaeoclimatology in mainland Australia. We clearly demonstrate that tree rings of *C. columellaris* provide new opportunities to develop long records of past rainfall and its variability. The Lake Tay chronology was positively and strongly correlated with autumn–winter rainfall, reflecting the relationship between rainfall and soil water availability and the importance of both the amount and variability of water availability for growth processes in semi-arid environments. The autumn–winter period is when the southern region receives much of its rainfall (around 70%) and it is unsurprising that rainfall during this time is a significant influence on tree growth. Autumn–winter rainfall in southern Western Australia is generally associated with both low pressure systems (cold

**Fig. 6** The MTM spectrum of (a) actual and (b) reconstructed rainfall over their common period (1902–2005) and (c) reconstructed rainfall over 1655–2005 with the 90, 95 and 99% confidence levels projected by robust estimation of the red-noise background spectrum. The periodicities of significant peaks are indicated above the spectral plot



fronts) in the midlatitude zone (40° to 50°S) and north-west cloud bands, which form east of a large trough off the coast of Western Australia as warm, moist subtropical air moves south-west and ascends.

Few other studies have developed tree-ring width chronologies from *Callitris*, even fewer have undertaken analysis of the climate signals retained by these chronologies and none have attempted to reconstruct rainfall using modern dendrochronological methods. We found a correlation of  $-0.39$  between summer (January–February) rainfall and a  $\delta^{18}\text{O}$  chronology developed from *C. columellaris* in the Pilbara, north-western Australia (Cullen and Grierson 2007). Baker et al. (2008), in an investigation of the dendroclimatic potential of *C. intratropica* in northern Australia, reported a correlation of 0.53 between a chronology developed from a 45 year old plantation and rainfall in the early part of the monsoon season (October–December). Chronologies developed from *Taxodium distichum* in south-eastern USA explained 54–68% of observed variation in spring rainfall (Stahle and Cleaveland 1994). Similarly, the two species commonly used to reconstruct rainfall and drought in North America, *Pseudotsuga menziesii* and *Pinus ponderosa*, typically capture 50–60% of variation in seasonal or annual rainfall (e.g. González-Elizondo et al. 2005; Watson and Luckman 2001, 2004). However, several studies have developed reconstructions using models where <40% of rainfall variation was related to growth (e.g. Buckley et al. 2004; Case and MacDonald 1995). In contrast, our model to predict past rainfall using tree rings explained 54% of variation in regional rainfall and compares favorably to other dendrochronological studies focused on reconstructing rainfall.

#### 4.1 Multi-decadal variability in rainfall over the last 350 years

Our reconstruction of autumn–winter rainfall reveals that rainfall in our study area has varied at the multi-decadal scale over the last 350 years. Reconstructed rainfall exhibits fluctuations from dry periods that often last 20–30 years to periods of above average rainfall that tend to persist for only 15 years or so. Spectral analysis of the reconstructed rainfall series provides further evidence for multi-decadal periodicities in rainfall in the region, with a spectral density peak at around 26–28 years. We believe these periodicities reflect real low frequency variability in rainfall (Rodionov 2006), but further efforts to develop an even longer chronology and chronologies from nearby regions are needed to confirm this belief. In addition, and although our reconstruction does not capture the full range of natural variability in rainfall, because of the limitations inherent in using regression analysis to (back) predict data, our data are consistent with climate modelling studies for the wider

region. Simulations of winter (June–August) rainfall over SWWA using the CSIRO Mark 3 climate model (Gordon et al. 2002), run over both a 100 and 500 year period, found that modeled rainfall exhibited drying trends lasting 20–30 years (Cai et al. 2005; IOCI 2005).

There is increasing evidence that sustained dry periods are a natural part of the rainfall regime for southern Western Australia; however, the drivers of this variation remain unclear. In the CSIRO Mark 3 model, cycles in rainfall were found to be an expression of variation in high-intensity rainfall events associated with inter-decadal variability in SAM, the principle mode of variability in Southern Hemisphere climate (Cai et al. 2005). Moreover, the decline in rainfall in recent decades coincides with an upward trend in SAM since 1965 (Li et al. 2005). Alternatively, Samuel et al. (2006) considered that the decline in rainfall was associated with a large-scale climatic shift over the southern and western Indian Ocean, evident as a switch from negative to positive SSTs around 1970.

In contrast, we found little evidence to support a connection between winter rainfall in the Lake Tay region and SAM or Indian Ocean SSTs: correlations between our tree-ring chronology and these climate indices were weak. In the case of SAM, the weak correlations might be due to the relative shortness of the observational records (<60 years). On the other hand, the weak correlation between tree rings and Indian Ocean SSTs could reflect a lack of a direct connection between the Indian Ocean and rainfall in our study area: the physical mechanism by which Indian Ocean SSTs might affect rainfall in SWWA, let alone the wider southern Western Australia region, is not yet understood (Samuel et al. 2006). We expect that future studies using tree rings of *Callitris* might be able to contribute more directly to questions about long term climate variability in the SWWA proper.

Our data suggests long-term, natural variation in rainfall in our study area is more likely to be due to low-frequency variation in the ENSO, one of the largest sources of natural variability in global climates (Allan et al. 1996). We found a significant, albeit relatively weak, positive correlation between the Lake Tay chronology and the Climatic Research Unit's SOI, a commonly used measure of ENSO. Many other studies have shown that ENSO affects rainfall in Australia, including southern Western Australia, with lower rainfall when the SOI is negative (Nicholls et al. 1996). Furthermore, the spectral peaks evident in the 2–4 year period in our rainfall reconstruction (and actual rainfall series) are consistent with the well-recognised periodicities in ENSO, which occur at 2.0–2.2 and 4.3 years (Jiang et al. 1995). However, ENSO also contains an inter-decadal component (Allan et al. 1996). Although the drivers of such low-frequency variation in ENSO are not yet fully understood, the impact of ENSO on

Australia's climate appears to be modulated by the Inter-decadal Pacific Oscillation, or IPO (Power et al. 1999). The IPO is an index of sea surface temperatures over the Pacific Ocean and cycles over a 15–30 year period (Power et al. 1999), consistent with cycles in tree growth apparent in our study. Future studies aimed at exploring the relationship between large-scale atmospheric modes such as ENSO and IPO, and tree growth of *Callitris* have potential to help determine the underlying causes of multi-decadal variation in rainfall in southern Western Australia.

## 5 Conclusion

The south-west region of Australia is currently experiencing a sustained decline in rainfall, as are many other regions of the world. Understanding low-frequency (inter-decadal and longer) variability in climate is the key to disentangling human-induced climate change from natural climate variation. However, much of our understanding of rainfall variability for the southern hemisphere in particular comes from short observational records (<100 years) and climate modelling studies. Our reconstruction of autumn–winter rainfall for a local region of southern Western Australia indicates that, over the last 350 years, rainfall has naturally varied from relatively dry periods lasting to 20–30 years to 15-year long periods of above average rainfall. Furthermore, these low frequency cycles in rainfall may be a reflection of variability in ENSO, although further exploration of the relationships between ENSO and tree growth is required.

**Acknowledgments** This work was supported by the Hermon Slade Foundation. Thank-you to Mathias Boer, Tim Langlois and two referees for their helpful comments that substantially improved our manuscript.

## References

- Allan R, Lindesay J, Parker D (1996) El Niño southern oscillation and climatic variability. CSIRO, Melbourne
- Ansell TJ, Reason CJC, Smith IN, Keay K (2000) Evidence for decadal variability in southern Australian rainfall and relationships with regional pressure and sea surface temperatures. *Int J Climatol* 20:1113–1129. doi:10.1002/1097-0088(200008)20:10<1113::AID-JOC531>3.0.CO;2-N
- Ash J (1983) Tree rings in tropical *Callitris macleayana* F. Muell *Aust J Bot* 31:277–281. doi:10.1071/BT9830277
- Baker PJ, Palmer JG, D'Arrigo RD (2008) The dendrochronology of *Callitris intratropica* in northern Australia: annual ring structure, chronology development and climate correlations. *Aust J Bot* 56:311–320. doi:10.1071/BT08040
- Biondi F, Waikul K (2004) DENDROCLIM2002: a C++ program for statistical calibration of climate signals in tree-ring chronologies. *Comput Geosci* 30:303–311. doi:10.1016/j.cageo.2003.11.004
- Briffa KR (1984) Tree-climate relationships and dendroclimatological reconstruction in the British Isles. PhD thesis, University of East Anglia
- Buckley BM, R.J.S. W, Kelly PE, Larson DW, Cook ER (2004) Inferred summer precipitation for southern Ontario back to AD 610, as reconstructed from ring widths of *Thuja occidentalis*. *Can J Res* 34:2541–2553. doi:10.1139/x04-129
- Bureau of Meteorology (2001) Australia's global climate observing system. Bureau of Meteorology, Melbourne
- Cai W, Shi G, Li Y (2005) Multidecadal fluctuations of winter rainfall over southwest Western Australia simulated in the CSIRO mark 3 coupled model. *Geophys Res Lett* 32:L12701. doi:10.1029/2005GL022712
- Cai WJ, Whetton PH, Karoly DJ (2003) The response of the Antarctic oscillation to increasing and stabilized atmospheric CO<sub>2</sub>. *J Clim* 16:1525–1538
- Case RA, MacDonald GM (1995) A dendroclimatic reconstruction of annual precipitation on the Western Canadian Prairies since A.D. 1505 from *Pinus flexilis* James. *Quat Res* 44:267–275. doi:10.1006/qres.1995.1071
- Cook ER (1985) A time series approach to tree ring standardization. PhD thesis, University of Arizona
- Cook ER, Briffa K (1990) Data analysis. In: Cook ER, Kairiukstis LA (eds) *Methods of dendrochronology*. International Institute for Applied Systems Analysis, Netherlands, pp 97–162
- Cook ER, Briffa K, Jones PD (1994) Spatial regression methods in dendroclimatology: a review and comparison of two techniques. *Int J Climatol* 14:379–402. doi:10.1002/joc.3370140404
- Cook ER, Krusic PJ (2006) ARSTAN40c. tree-ring laboratory, Lamont-Doherty earth observatory, New York. Available from <http://www.ldeo.columbia.edu/res/fac/trl/public/publicSoftware.html>
- Cook ER, Peters K (1997) Calculating unbiased tree-ring indices for the study of climatic and environmental change. *Holocene* 7:361–370. doi:10.1177/095968369700700314
- CSIRO (2001) Climate change: projections for Australia. CSIRO Climate Impact Group, Aspendale
- Cullen LE, Grierson PF (2006) Is cellulose extraction necessary for developing stable carbon and oxygen isotope chronologies from *Callitris glaucophylla*?. *Palaeogeogr Palaeoclimatol Palaeoecol* 236:206–216. doi:10.1016/j.palaeo.2005.11.003
- Cullen LE, Grierson PF (2007) A stable oxygen, but not carbon, isotope chronology of *Callitris columellaris* reflects recent climate change in north-western Australia. *Clim Change* 85:213–229. doi:10.1007/s10584-006-9206-3
- Durbin J, Watson GS (1951) Testing for serial correlation in least squares regression, II. *Biometrika* 38:159–179
- Farjon A (2005) A monograph of Cupressaceae and Sciadopityae. Royal Botanic Gardens, Kew
- Frederiksen JS, Frederiksen C (2005) Decadal changes in Southern Hemisphere winter cyclogenesis. CSIRO Marine and Atmospheric Research, Aspendale
- Fritts HC (1976) *Tree rings and climate*. Academic Press, London
- Fritts HC, Guiot J, Gordon GA, Schweingruber F (1990) Methods of calibration, verification, and reconstruction. In: Cook ER, Kairiukstis LA (eds) *Methods of dendrochronology*. International Institute for Applied Systems Analysis, Netherlands, pp 163–217
- González-Elizondo M, Jurado E, Návaz J, González-Elizondo MS, Villanueva J, Aguirre O, Jiménez J (2005) Tree-rings and climate relationships for Douglas-fir chronologies from the Sierra Madre Occidental, Mexico: a 1681–2001 rain reconstruction. *For Ecol Manage* 213:39–53
- Gordon HB, Rotstayn LD, McGregor JL et al (2002) The CSIRO Mk3 climate system model. CSIRO Division of Atmospheric Research, Aspendale
- Graham NE, Hughes MK, Ammann CM et al (2007) Tropical Pacific—mid-latitude teleconnections in medieval times. *Clim Change* 83:241–285. doi:10.1007/s10584-007-9239-2

- Graumlich LJ (1991) Subalpine tree growth, climate, and increasing CO<sub>2</sub>: an assessment of recent growth trends. *Ecol* 72:1–11. doi:10.2307/1938895
- Hennessy KJ, Suppiah R, Page CM (1999) Australian rainfall changes, 1910–1999. *Aust Meteorol Mag* 48:1–13
- Holmes R (1983) Computer-assisted quality control in tree-ring dating and measurement. *Tree-Ring Bull* 43:69–78
- IOCI (2002) Climate variability and change in south west Western Australia. Indian Ocean Climate Initiative Panel, Perth
- IOCI (2005) Indian Ocean climate initiative stage 2: report of phase 1 activity. Indian Ocean Climate Initiative Panel, Perth
- Jiang N, Neelin JD, Ghil M (1995) Quasi-quadrinial and quasi-biennial variability in the equatorial Pacific. *Clim Dyn* 12:101–112. doi:10.1007/BF00223723
- Jones PD, Briffa KR, Barnett TP, Tett SFB (1998) High-resolution palaeoclimatic records for the last millennium: interpretation, integration and comparison with general circulation model control-run temperatures. *Holocene* 8:455–471. doi:10.1191/095968398667194956
- Knapp PA, Soulé PT, Grissino-Mayer HD (2001) Detecting potential regional effects of increased atmospheric CO<sub>2</sub> on growth rates of western juniper. *Glob Chang Biol* 7:903–917. doi:10.1046/j.1365-2486.2001.00452.x
- Kushner PJ, Held IM, Delworth TL (2001) Southern Hemisphere atmospheric circulation response to global warming. *J Clim* 14:2238–2249. doi:10.1175/1520-0442(2001)014<0001:SHACRT>2.0.CO;2
- LaMarche VC, Holmes R, Dunwiddie PW, Drew LG (1979) Tree-ring chronologies of the Southern Hemisphere 4. Australia. Laboratory of tree-ring research, University of Arizona
- Lange RT (1965) Growth ring characteristics in an arid zone conifer. *Trans R Soc S Aust* 89:133–137
- Lawrence DM, Grissino-Mayer HD (2001) Verify for windows. Available from <http://fuzzo.com/science/verify.htm>
- Li Y, Cai W, Campbell EP (2005) Statistical modeling of extreme rainfall in southwest Western Australia. *J Clim* 18:852–863. doi:10.1175/JCLI-3296.1
- Lough JM (2007) Tropical river flow and rainfall reconstructions from coral luminescence: Great Barrier Reef, Australia. *Paleoceanography* 22. doi:10.1029/2006PA001377
- MacDonald GM, Sziecz JM, Claricoates J, Dale KA (1998) Response of the Central Canadian treeline to recent climatic changes. *Ann Assoc Am Geogr* 88:183–208. doi:10.1111/1467-8306.00090
- Mann ME, Lees JM (1996) Robust estimation of background noise and signal detection in climatic time series. *Clim Change* 33:409–445. doi:10.1007/BF00142586
- Marshall GJ (2003) Trends in the southern annular mode from observations and reanalyses. *J Clim* 16:4134–4143
- New M, Todd M, Hulme M, Jones P (2001) Precipitation measurements and trends in the twentieth century. *Int J Climatol* 21:1889–1922. doi:10.1002/joc.680
- Nicholls N, Lavery B (1992) Australian rainfall trends during the twentieth century. *Int J Climatol* 12:153–163. doi:10.1002/joc.3370120204
- Nicholls N, Lavery B, Frederiksen C, Drosowsky W (1996) Recent apparent changes in relationships between the El Niño—southern oscillation and Australian rainfall and temperature. *Geophys Res Lett* 23:3357–3360. doi:10.1029/96GL03166
- Osborn TJ, Briffa K, Jones PD (1997) Adjusting variance for sample size in tree-ring chronologies and other regional mean timeseries. *Dendrochron* 15:89–99
- Perkins JE (1986) The dendrochronology of *Callitris columellaris* F. Muell. in arid, sub-tropical continental Western Australia. M.A. thesis, University of Western Australia
- Pittock B (2003) Climate change: an Australian guide to the science and potential impacts. Australian Greenhouse Office, Canberra
- Power S, Casey T, Folland C, Colman A, Mehta V (1999) Interdecadal modulation of the impact of ENSO on Australia. *Clim Dyn* 15:319–324. doi:10.1007/s003820050284
- Rodionov SN (2006) Use of prewhitening in climate regime shift detection. *Geophys Res Lett* 33:L12707. doi:10.1029/2006GL025904
- Ropelewski CF, Jones PD (1987) An extension of the Tahiti–Darwin southern oscillation index. *Mon Weather Rev* 115:2161–2165. doi:10.1175/1520-0493(1987)115<2161:AEOTTS>2.0.CO;2
- Samuel JM, Verdon DC, Sivapalan M, Franks SW (2006) Influence of Indian Ocean sea surface temperature variability on southwest Western Australian winter rainfall. *Water Res Bull* 42:W08402 doi:10.1029/2005WR004672
- Sarris D, Christodoulakis D, Korner C (2007) Recent decline in precipitation and tree growth in the eastern Mediterranean. *Glob Chang Biol* 13:1187–1200. doi:10.1111/j.1365-2486.2007.01348.x
- Seager R, Graham N, Herweijer C, Gordon AL, Kushnir Y, Cook E (2007) Blueprints for medieval hydroclimate. *Quat Sci Rev* 26:2322–2336. doi:10.1016/j.quascirev.2007.04.020
- Smith IN (2004) An assessment of recent trends in Australian rainfall. *Aust Metab Mag* 53:163–173
- Smith IN, McIntosh PD, Ansell TJ, Reason CJC, McInnes K (2000) Southwest Western Australia winter rainfall and its association with Indian Ocean climate variability. *Int J Climatol* 20:1913–1930. doi:10.1002/1097-0088(200012)20:15<1913::AID-JOC594>3.0.CO;2-J
- Solomon S, Qin D, Manning M et al (2007) Climate change 2007: the physical science basis. Contribution of working group I to the fourth assessment report of the intergovernmental panel on climate change. Cambridge University Press, Cambridge
- Stahle DW, Cleaveland MK (1994) Tree-ring reconstructed rainfall over the southeastern USA during the medieval warm period and little ice age. *Clim Change* 26:199–212. doi:10.1007/BF01092414
- Thomson DJ (1982) Spectrum estimation and harmonic analysis. *IEEE Proc* 70:1055–1096. doi:10.1109/PROC.1982.12433
- Treble PC, Chappell J, Gagan MK, McKeegan KD, Harrison TM (2005) In situ measurements of seasonal δ<sup>18</sup>O variations and analysis of isotopic trends in a modern speleothem from southwest Australia. *Earth Planet Sci Lett* 233:17–32. doi:10.1016/j.epsl.2005.02.013
- Treble PC, Shelley JMG, Chappell J (2003) Comparison of high resolution sub-annual records of trace elements in a modern (1911–1992) speleothem with instrumental climate data from southwest Australia. *Earth Planet Sci Lett* 216:141–153. doi:10.1016/S0012-821X(03)00504-1
- Treydte KS, Schleser GH, Helle G, Frank DC, Winiger M, Haug GH et al (2006) The twentieth century was the wettest period in northern Pakistan over the past millennium. *Nature* 440:1179–1182. doi:10.1038/nature04743
- Watson E, Luckman BH (2001) Dendroclimatic reconstruction of precipitation for sites in the southern Canadian Rockies. *Holocene* 11:203–213. doi:10.1191/095968301672475828
- Watson E, Luckman BH (2004) Tree-ring based reconstructions of precipitation for the southern Canadian Cordillera. *Clim Change* 65:209–241. doi:10.1023/B:CLIM.0000037487.83308.02
- Wigley TML, Briffa KR, Jones PD (1984) On the average value of correlated time series, with application in dendroclimatology and hydrometeorology. *J Clim Appl Meteorol* 23:201–213. doi:10.1175/1520-0450(1984)023<0201:OTAVOC>2.0.CO;2